Chinese Chemical Letters 34 (2023) 108244

Contents lists available at ScienceDirect

Chinese Chemical Letters

journal homepage: www.elsevier.com/locate/cclet

Spectroscopic identification of water splitting by neutral group 3 metals

Shuai Jiang[a,b], Huijun Zheng[b,c], Wenhui Yan[b,c], Tiantong Wang[b,c], Chong Wang[b,c], Ya Zhao[b], Hua Xie[b], Gang Li[b,*], Xiucheng Zheng[a,*], Hongjun Fan[b,*], Ling Jiang[b,*]

[a] College of Chemistry, Zhengzhou University, Zhengzhou 450001, China
[b] State Key Laboratory of Molecular Reaction Dynamics, Dalian Institute of Chemical Physics, Chinese Academy of Sciences, Dalian 116023, China
[c] University of Chinese Academy of Sciences, Beijing 100049, China

ARTICLE INFO

Article history:
Received 11 November 2022
Revised 10 January 2023
Accepted 16 February 2023
Available online 19 February 2023

Keywords:
Water splitting
Cluster
Group 3 metals
Infrared spectroscopy
Quantum chemical calculations

ABSTRACT

Spectroscopic study of water splitting by neutral metal clusters is crucial to understanding the microscopic mechanism of catalytic processes but has been proven to be a challenging experimental target due to the difficulty in size selection. Here, we report a size-specific infrared spectroscopic study of the reactions between neutral group 3 metals and water molecules based on threshold photoionization using a vacuum ultraviolet laser. Quantum chemical calculations were carried out to identify the structures and to assign the experimental spectra. All the $M_2O_4H_4$ (M = Sc, Y, La) products are found to have the intriguing $M_2(\mu_2\text{-O})(\mu_2\text{-H})(\mu_2\text{-OH})(\eta^1\text{-OH})_2$ structures, indicating that the H–OH bond breaking, the M–O/M–H/M–OH bond formation, and hydrogen production proceed efficiently in the reactions between laser-vaporized metals and water molecules. The joint experimental and theoretical results on the atomic scale demonstrate that the water splitting by neutral group 3 metals is both thermodynamically exothermic and kinetically facile in the gas phase. These findings have important implications for unravelling the structure-reactivity relationship of catalysts with isolated metal atoms/clusters dispersed on supports.

Water splitting is regarded as one of the most promising technologies for renewable sources, transport, and storage of hydrogen energy [1–3]. The process of water splitting involves the breaking/formation of chemical bonds and hydrogen production. The investigation of the reactions between metals and water molecules helps to uncover the microscopic mechanisms of catalytic processes with isolated metal atoms/clusters dispersed on supports [4–7]. Over the past several decades, extensive efforts were devoted to the spectroscopic studies of ionic metals with water molecules, which allow easy size selection and detection [8–11]. In general, the water molecules are weakly coordinated to the metal ions, forming the solvation structures in the form of $M^+(H_2O)_n$ [12]. The $HMOH^+(H_2O)_n$ insertion complexes were observed for some metal atoms [13–17]. For instance, infrared multiple photon dissociation spectroscopy showed that $Mn^+(H_2O)_n$ (n = 4-8) undergoes an insertion reaction forming $HMnOH^+(H_2O)_{n-1}$ [17].

For the reactions between neutral metal atoms and water molecules, the HMOH intermediates were observed for early transition metal atoms and could either photochemically isomerize to H_2MO or decompose to metal monoxides and H_2 [18–23]. The late transition metal and lanthanide metal atoms react with H_2O to produce the solvated $M(H_2O)$ complexes, which are rearranged to the insertion complexes under UV irradiation [24–28]. For the actinide metal atoms, the thorium and uranium atoms are able to insert into the O–H bond of water to form the H_2ThO and H_2UO molecules [29,30]. Along with significant advances in theoretical calculations, these studies provided great insights into the reaction mechanisms of metal atoms with water. Thus far, spectroscopic studies on the reactions of neutral metal clusters with water are rather challenging experimentally, because the absence of a charge makes for difficult size selection and detection. Here we report an infrared-vacuum ultraviolet (IR-VUV) spectroscopic study on the reactions of neutral group 3 metals with water molecules. IR-VUV spectroscopy in conjunction with quantum chemical calculations confirm that all the neutral $M_2O_4H_4$ (M = Sc, Y, La) complexes have unexpected $M_2(\mu_2\text{-O})(\mu_2\text{-H})(\mu_2\text{-OH})(\eta^1\text{-OH})_2$ structures, demonstrating that the H–OH bond breaking, the M–O/M–H/M–OH bond formation, and hydrogen production proceed efficiently in the reactions between laser-vaporized metals and water molecules.

The experimental IR spectra were measured using an IR-VUV spectroscopy apparatus (see Supporting information for experimental details) [31,32]. Neutral $M_2O_4H_4$ (M = Sc, Y, La) complexes

* Corresponding authors.
E-mail addresses: gli@dicp.ac.cn (G. Li), zhxch@zzu.edu.cn (X. Zheng), fanhj@dicp.ac.cn (H. Fan), ljiang@dicp.ac.cn (L. Jiang).

https://doi.org/10.1016/j.cclet.2023.108244
1001-8417/

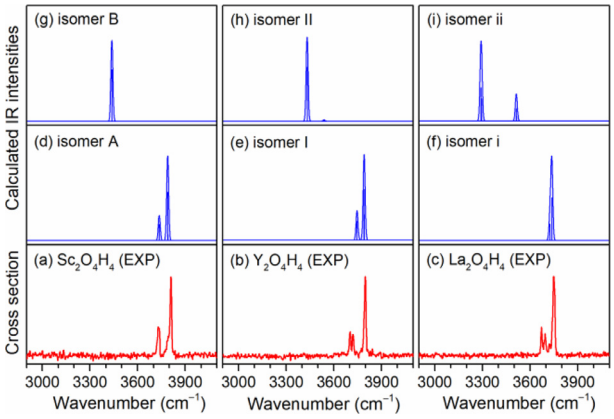

Fig. 1. Comparison of experimental IR spectra (a–c) of neutral $M_2O_4H_4$ (M = Sc, Y, La) complexes and calculated IR spectra (d–i) of the two types of isomers.

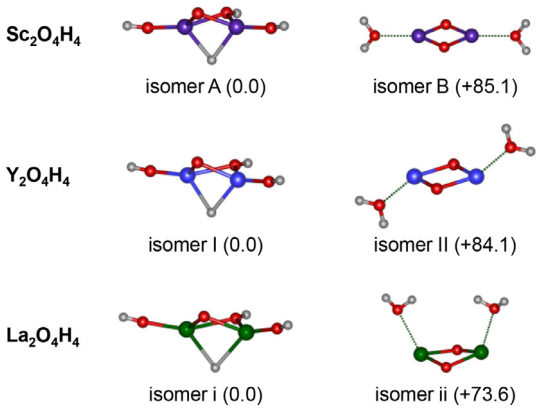

Fig. 2. Optimized structures of the two types of isomers of neutral $M_2O_4H_4$ (M = Sc, Y, La) complexes (O, red; H, light gray; Sc, purple; Y, blue; La, olive). Relative energies (in parenthesis) are listed in kcal/mol.

Table 1
Comparison of the experimental band positions (cm^{-1}) of neutral $M_2O_4H_4$ (M = Sc, Y, La) complexes to the calculated values of the most stable structures (isomers A, I and i) obtained at the B3LYP/aug-pVTZ(O, H)/SDD(Sc, Y, La) level of theory (IR intensities are listed in parentheses in km/mol, and the calculated harmonic vibrational frequencies are scaled by a factor of 0.962).

Species	Exptl.	Calcd.	Mode
$Sc_2O_4H_4$	3729	3736 (90)	OH stretching mode
	3809	3789 (272)	Antisymmetric OH stretching mode
		3790 (33)	Symmetric OH stretching mode
$Y_2O_4H_4$	3721	3746 (67)	OH stretching mode
	3799	3791 (182)	Antisymmetric OH stretching mode
		3791 (14)	Symmetric OH stretching mode
$La_2O_4H_4$	3683	3725 (43)	OH stretching mode
	3749	3737 (113)	Antisymmetric OH stretching mode
		3737 (22)	Symmetric OH stretching mode

were prepared *via* laser vaporization in a supersonic expansion of 0.1% H_2O/helium. For the IR excitation of neutral $M_2O_4H_4$ complexes, we used a tunable IR optical parametric oscillator/optical parametric amplifier system (LaserVision). Subsequent photoionization was carried out with about 65 ns delay with a VUV light at 193 nm. IR spectra were recorded in the difference mode of operation (IR laser on IR laser off). IR power dependence of the signal was measured to ensure that the predissociation yield was linear with photon flux.

The experimental IR spectra of $M_2O_4H_4$ (M = Sc, Y, La) in the OH stretching region are shown in Figs. 1a–c and the band positions are listed in Table 1. The IR spectrum of each individual $M_2O_4H_4$ complex consists of two groups of bands, centering at 3729/3809 cm^{-1} (Sc), 3721/3799 cm^{-1} (Y) and 3683/3749 cm^{-1} (La), respectively. The gap between the two experimental bands for $M_2O_4H_4$ (M = Sc, Y, La) is 80, 78 and 66 cm^{-1}, respectively, indicating a monotonical decease down through the group 3 of the periodic table. Such gaps are smaller than that between the symmetric and antisymmetric OH stretching vibrational frequencies of the free water molecule (99 cm^{-1}) [33].

To understand the experimentally observed spectral features and identify the structures of the $M_2O_4H_4$ (M = Sc, Y, La) complexes, quantum chemical calculations were carried out at the B3LYP/aug-pVTZ(O, H)/SDD(Sc, Y, La) level of theory (see Supporting information for theoretical details). Relative energies and energy barriers include the zero-point energy corrections. The optimized structures of the two types of isomers are shown in Fig. 2. The calculated IR spectra are compared with the experimental ones in Fig. 1.

For each of $M_2O_4H_4$ (M = Sc, Y, La), the most stable isomer has a $M_2(\mu_2\text{-O})(\mu_2\text{-H})(\mu_2\text{-OH})(\eta^1\text{-OH})_2$ configuration with a singlet electronic ground state (labeled isomers A, I and i in Fig. 2), forming an insertion structure. In the second type of isomer (labeled isomers B, II and ii in Fig. 2), the water molecules are weakly bound to the metal atoms of the rhombus $M_2(\mu_2\text{-O})_2$ unit, forming a solvation structure. Isomers B, II and ii lie much higher in energy than isomers A, I and i by 85.1, 84.1 and 73.6 kcal/mol, respectively, indicating that these water-solvated structures are thermodynamically unstable as compared to the insertion structures.

In the simulated IR spectrum of isomer A of $Sc_2O_4H_4$ (Fig. 1d), the band at 3736 cm^{-1} is attributed to the OH stretching mode of the bridging OH group, which is consistent with the experimental band of 3729 cm^{-1} (Table 1); the antisymmetric and symmetric OH stretching modes of the terminal OH groups are calculated to 3789 and 3790 cm^{-1}, respectively, which are in agreement with the experimental band of 3809 cm^{-1}. The simulated IR spectrum of isomer B of $Sc_2O_4H_4$ (Fig. 1g) exhibits a single band at 3438 cm^{-1}, which is not observed experimentally. It thus appears that isomer B does not contribute to the experimental spectrum of $Sc_2O_4H_4$. Similar results are also obtained for the $Y_2O_4H_4$ and $La_2O_4H_4$ complexes. The calculated band gap between the OH and antisymmetric/symmetric OH stretching modes of isomers A, I, and i is 53, 45 and 12 cm^{-1}, respectively, which trend is in accordance with the experimental trend. Note that the predicted band gaps are systematically smaller than the experimental values, which may be attributed to the deficiencies of theoretical methods. The decease of the band gap between the bridging and terminal OH stretching modes for $M_2O_4H_4$ (M = Sc, Y, La) might be rationalized by the reduced electronegativities down through the group 3 of the periodic table. The Pauling electronegativity of Sc, Y and La is 1.36, 1.22 and 1.10, respectively. The charge transfer from the metal to the OH group weakens the O–H bond and reduces the frequency of its vibrational mode [12]. Furthermore, the O–H bond in the monodentate terminal OH group is more strongly influenced by binding to the metal center than that in the bidentate bridging OH group, resulting in a larger red-shift of stretching vibrational frequency (Table 1). Overall, the agreement of the simulated IR spectra of isomers A, I and i with experiment is reasonable to confirm the assignment of these insertion structures responsible for the experimental spectra.

The most striking observation in the present work is the identification of the $M_2(\mu_2\text{-O})(\mu_2\text{-H})(\mu_2\text{-OH})(\eta^1\text{-OH})_2$ structures instead of the water-solvated motifs. The results suggest that the H–OH bond breaking and M–O/M–H/M–OH bond formation proceed in the reactions between laser-vaporized metals and water molecules.

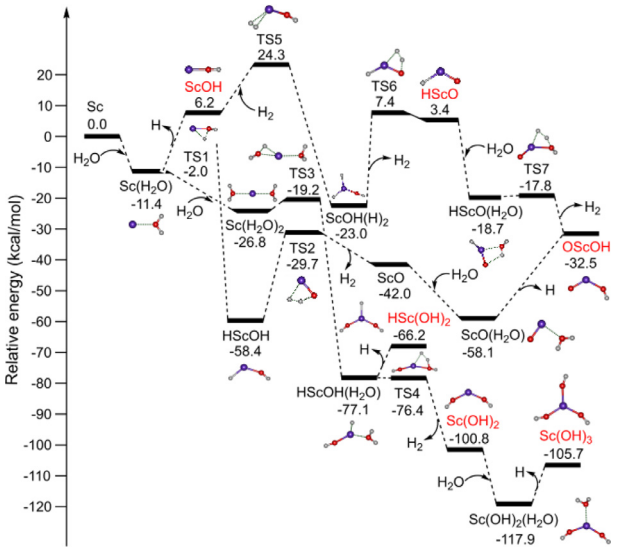

Fig. 3. Potential energy profiles for the formation of mononuclear complexes. The abbreviation "IM" stands for intermediate and "TS" for transition state. The corresponding structures are embedded in the inset (O, red; H, light gray; Sc, purple). The complexes dedicated to the formation of target product are marked with red color.

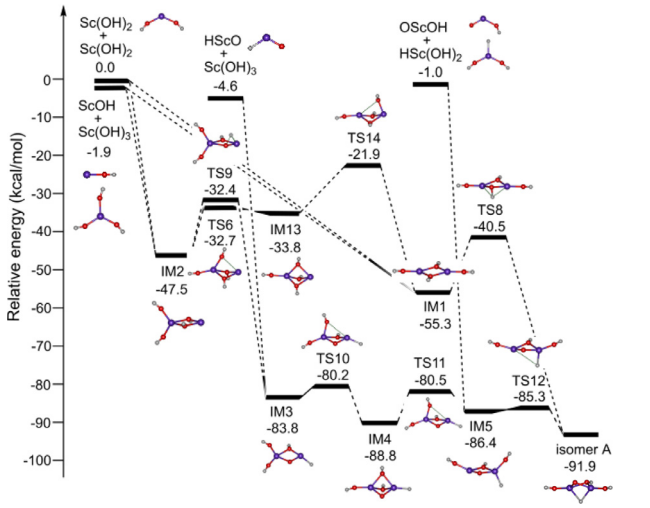

Fig. 4. Potential energy profiles for the formation of target product ($Sc_2O_4H_4$, isomer A). The abbreviation "IM" stands for intermediate and "TS" for transition state. The corresponding structures are embedded in the inset (O, red; H, light gray; Sc, purple).

Note that the reaction processes taking place in the plasma conditions in the laver-vaporization source are quite complicated and are very difficult to be clearly characterized, quantum chemical calculations were performed to explore the possible reaction mechanisms.

Due to the spectra and structural similarity of $M_2O_4H_4$ among the group 3 metals, we will focus on the discussion of formation mechanisms of $Sc_2O_4H_4$. The potential energy profiles for the reactions between Sc atoms and water molecules were calculated at the B3LYP/aug-pVTZ(O, H)/SDD(Sc) level of theory. The reaction (1) is predicted to be exothermic by 11.4 kcal/mol, whereas the reaction (2) is exothermic by 7.3 kcal/mol [34]. This implies that the initial reaction of Sc with H_2O to form $Sc(H_2O)$ is more favorable than the dimerization of Sc atoms.

$$Sc + H_2O \rightarrow Sc(H_2O) \quad (1)$$

$$Sc + Sc \rightarrow Sc_2 \quad (2)$$

As shown in Fig. 3, the isomerization from $Sc(H_2O)$ to HScOH is highly exothermic by 47.0 kcal/mol *via* a transition state (TS1) with a small barrier of 9.4 kcal/mol. HScOH could release H_2 to produce ScO *via* TS2. TS1 and TS2 lies below the energy of $Sc + H_2O$ reactants by 2.0 and 29.7 kcal/mol, respectively. The $Sc + H_2O \rightarrow ScO + H_2$ overall reaction is exothermic by 42.0 kcal/mol and is thus thermodynamically favorable. Indeed, the ScO^+ species is observed in the mass spectra (Fig. S1 in Supporting information). This water splitting by Sc atom is supported by the absence of water-solvated structures in the present IR-VUV and previous matrix-isolation experiments [19,20].

The addition of H_2O to ScO forms $ScO(H_2O)$, which is exothermic by 16.1 kcal/mol. Although the dehydrogenation of $ScO(H_2O)$ is endothermic by 25.6 kcal/mol, this entropy-driven reaction might be feasible in the high-temperature plasma environments. On the other hand, OScOH lies energetically below the reactants by 32.5 kcal/mol, indicating that the formation of OScOH is thermodynamically favored. The addition of H_2O to $Sc(H_2O)$ yields $Sc(H_2O)_2$, which could undergo isomerization and dehydrogenation to generate $HSc(OH)_2$. These processes are predicated to be both thermodynamically exothermic and kinetically facile. The $HScOH(H_2O)$ complex could undergo H_2 production to form $Sc(OH)_2$, which is exothermic by 23.7 kcal/mol with a very small barrier of 0.7 kcal/mol (TS4). The $Sc(OH)_3$ complex might be formed *via* the addition of the third water molecule to $Sc(OH)_2$ and the subsequent dehydrogenation. The $Sc(OH)_n$ (n = 1-3) complexes might also be produced by the reactions of Sc atoms with OH radicals as proposed previously [19]. Although the barrier for the $ScOH \rightarrow HScO$ isomerization is very high (30.4 kcal/mol), the strong exothermic property of the $Sc + OH \rightarrow HScO$ overall reaction suggests that this process is thermodynamically favorable. Alternatively, the formation of HScO could be assisted by the H_2 addition to ScOH. The MO, HMO, $M(OH)_{1,2}$ and $HM(OH)_{1,2}$ (M = Sc, Y, La) complexes were captured from the reactions between laser-vaporized metal atoms and water molecules in rare-gas matrixes [18–20], which support the aforementioned mechanisms.

As shown in Fig. 4, the dimerization of $Sc(OH)_2$ produces the intermediate IM1, which is predicted to be highly exothermic by 55.3 kcal/mol. The combination of ScOH and $Sc(OH)_3$ generates the intermediate IM2, releasing the energy by 45.6 kcal/mol. The aggregation of ScH-containing fragments, $HScO + Sc(OH)_3$ and $OScOH + HSc(OH)_3$, is even more exothermic of 79.2 and 85.4 kcal/mol, yielding more stable intermediates IM3 and IM5. All the intermediates (IM1, IM2, IM3 and IM5) can be isomerized to the most stable structure of isomer A *via* several intermediates and transition states, with the largest barrier of ~15 kcal/mol. The potential energy profiles clearly demonstrate that the formation of isomer A is both thermodynamically exothermic and kinetically facile in the gas phase, indicating that the H–OH bond breaking, the M–O/M–H/M–OH bond formation, and hydrogen production proceed quite efficiently at the experimental conditions.

The above pathway for the formation of $Sc_2O_4H_4$ begins with the generation of mononuclear complexes from the reactions between Sc and H_2O (Fig. 3) and then proceeds with the aggregation of the relevant mononuclear complexes (Fig. 4). Such reaction mechanisms are not exclusive. For instance, the combination of Sc atoms with mononuclear complexes or the reaction of Sc_2 with H_2O to produce the binuclear complexes is also likely. As exemplified in Fig. S2 (Supporting information), the addition of Sc atom to the HScOH complex, resulting in the formation of $Sc_2(\mu_2\text{-H})(\mu_2\text{-OH})$. This binuclear complex could further undergo H_2O addition, isomerization, and H_2 production, leading to the formation of IM1. As shown in Fig. 4, the isomerization from IM1 to isomer A is both

thermodynamically exothermic and kinetically facile. As shown in Fig. S3 (Supporting information), the addition of H_2O to Sc_2 forms the $Sc_2(H_2O)$ adduct, which is exothermic by 12.2 kcal/mol. $Sc_2(H_2O)$ undergoes OH dissociation to produce $Sc_2(\mu_2\text{-H})(\eta^1\text{-OH})$, which is highly exothermic by 58.6 kcal/mol with a very small barrier of 4.3 kcal/mol (TS18). The isomerization from $Sc_2(\mu_2\text{-H})(\eta^1\text{-OH})$ to $Sc_2(\mu_2\text{-H})(\mu_2\text{-OH})$ is exothermic by 6.5 kcal/mol with a barrier of 5.8 kcal/mol (TS19). The subsequent reactions could proceed efficiently to reach the final product (Fig. S2). Since the reducibility of Y and La is stronger than that of Sc, the proposed mechanisms of $Sc_2O_4H_4$ would be more feasible for the formation of $Y_2O_4H_4$ and $La_2O_4H_4$ complexes.

In summary, the neutral $M_2O_4H_4$ (M = Sc, Y, La) complexes were prepared in the gas phase *via* laser vaporization technique. Infrared-vacuum ultraviolet (IR-VUV) spectroscopy in conjunction with quantum chemical calculations confirm that all of these complexes have $M_2(\mu_2\text{-O})(\mu_2\text{-H})(\mu_2\text{-OH})(\eta^1\text{-OH})_2$ structures. The results indicate that the H–OH bond breaking, the M–O/M–H/M–OH bond formation, and H_2 production proceed efficiently in the reactions between laser-vaporized metal atoms and water molecules. Theoretical calculations reveal that the formation of $M_2(\mu_2\text{-O})(\mu_2\text{-H})(\mu_2\text{-OH})(\eta^1\text{-OH})_2$ from the reaction of group 3 metals with water is both thermodynamically exothermic and kinetically facile in the gas phase. The present findings provide important insights into the structure-reactivity mechanism of metal clusters toward the water molecules and key microscopic information for systematic understanding of water splitting on the active sites of catalysts.

Declaration of competing interest

The authors declare that they have no known competing financial interests or personal relationships that could have appeared to influence the work reported in this paper.

Acknowledgments

The authors gratefully acknowledge the Dalian Coherent Light Source (DCLS) for support and assistance. This work was supported by the National Key Research and Development Program of China (No. 2021YFA1400501), the National Natural Science Foundation of China (Nos. 22125303, 92061203, 92061114, 21976049, 22103082, 22273101 and 22288201), the Youth Innovation Promotion Association of the Chinese Academy of Sciences (CAS) (No. 2020187), Innovation Program for Quantum Science and Technology (No. 2021ZD0303304), CAS (No. GJJSTD20220001), Dalian Institute of Chemical Physics (No. DICP DCLS201702), International Partnership Program of CAS (No. 121421KYSB20170012), and K.C. Wong Education Foundation (No. GJTD-2018-06).

References

[1] A. Fujishima, K. Honda, Nature 238 (1972) 37–38.
[2] A. Kudo, Y. Miseki, Chem. Soc. Rev. 38 (2009) 253–278.
[3] T. Takata, J. Jiang, Y. Sakata, et al., Nature 581 (2020) 411–414.
[4] U. Heiz, E.L. Bullock, J. Mater. Chem. 14 (2004) 564–577.
[5] B. Qiao, A. Wang, X. Yang, et al., Nat. Chem. 3 (2011) 634–641.
[6] I. Chakraborty, T. Pradeep, Chem. Rev. 117 (2017) 8208–8271.
[7] J.-C. Liu, Y. Tang, Y.-G. Wang, et al., Nat. Sci. Rev. 5 (2018) 638–641.
[8] A. Irigoras, J.E. Fowler, J.M. Ugalde, J. Am. Chem. Soc. 121 (1999) 574–580.
[9] T.D. Vaden, C.J. Weinheimer, J.M. Lisy, J. Chem. Phys. 121 (2004) 3102–3107.
[10] R.S. Walters, E.D. Pillai, M.A. Duncan, J. Am. Chem. Soc. 127 (2005) 16599–16610.
[11] J.U. Reveles, P. Calaminici, M.R. Beltran, et al., J. Am. Chem. Soc. 129 (2007) 15565–15571.
[12] N.R. Walker, R.S. Walters, M.A. Duncan, New J. Chem. 29 (2005) 1495–1503.
[13] J. Heller, W.K. Tang, E.M. Cunningham, et al., Angew. Chem. Int. Ed. 60 (2021) 16858–16863.
[14] J. Heller, T.F. Pascher, D. Muss, et al., Phys. Chem. Chem. Phys. 23 (2021) 22251–22262.
[15] J. Heller, T.F. Pascher, C. van der Linde, et al., Chem. Eur. J. 27 (2021) 16367–16376.
[16] J. Heller, E.M. Cunningham, J.C. Hartmann, et al., Phys. Chem. Chem. Phys. 24 (2022) 14699–14708.
[17] J. Heller, E.M. Cunningham, C. van der Linde, et al., J. Phys. Chem. Lett. 13 (2022) 3269–3275.
[18] J.W. Kauffman, R.H. Hauge, J.L. Margrave, J. Phys. Chem. 89 (1985) 3547–3552.
[19] L.N. Zhang, J. Dong, M.F. Zhou, J. Phys. Chem. A 104 (2000) 8882–8886.
[20] L.N. Zhang, L.M. Shao, M.F. Zhou, Chem. Phys. 272 (2001) 27–36.
[21] M.F. Zhou, L.N. Zhang, J. Dong, Q.Z. Qin, J. Am. Chem. Soc. 122 (2000) 10680–10688.
[22] M.F. Zhou, J. Dong, L.N. Zhang, Q.Z. Qin, J. Am. Chem. Soc. 123 (2001) 135–141.
[23] V.A. Macrae, A.J. Downs, Phys. Chem. Chem. Phys. 6 (2004) 4571–4578.
[24] J.W. Kauffman, R.H. Hauge, J.L. Margrave, J. Phys. Chem. 89 (1985) 3541–3547.
[25] M.F. Zhou, L.N. Zhang, L.M. Shao, et al., J. Phys. Chem. A 105 (2001) 5801–5807.
[26] L.N. Zhang, M.F. Zhou, L.M. Shao, et al., J. Phys. Chem. A 105 (2001) 6998–7003.
[27] J. Xu, M. Zhou, J. Phys. Chem. A 110 (2006) 10575–10582.
[28] J. Xu, X. Jin, M. Zhou, J. Phys. Chem. A 111 (2007) 7105–7111.
[29] B.Y. Liang, L. Andrews, J. Li, B.E. Bursten, J. Am. Chem. Soc. 124 (2002) 6723–6733.
[30] B. Liang, R.D. Hunt, G.P. Kushto, et al., Inorg. Chem. 44 (2005) 2159–2168.
[31] B. Zhang, Y. Yu, Z. Zhang, et al., J. Phys. Chem. Lett. 11 (2020) 851–855.
[32] G. Li, C. Wang, H.J. Zheng, et al., Chin. J. Chem. Phys. 34 (2021) 51–60.
[33] G. Herzberg, Infrared and Raman Spectra of Polyatomic Molecules, Molecular Spectra and Molecular Structure II, Van Nostrand and Co., Inc, Princeton, 1945.
[34] C. Camacho, H.A. Witek, R. Cimiraglia, J. Chem. Phys. 132 (2010) 244306.